IOPscience iopscience.iop.org

Home Search Collections Journals About Contact us My IOPscience

Effect of meibomian lipid layer on evaporation of tears

This article has been downloaded from IOPscience. Please scroll down to see the full text article.

2004 J. Phys.: Condens. Matter 16 S2461

(http://iopscience.iop.org/0953-8984/16/26/019)

View the table of contents for this issue, or go to the journal homepage for more

Download details:
IP Address: 129.252.86.83
The article was downloaded on 27/05/2010 at 15:41

Please note that terms and conditions apply.

INSTITUTE OF PHYSICS PUBLISHING JOURNAL OF PHYSICS: CONDENSED MATTER

J. Phys.: Condens. Matter **16** (2004) S2461–S2467 PII: S0953-8984(04)76238-4

Effect of meibomian lipid layer on evaporation of tears

F Miano[1], M Calcara[1], F Giuliano[1], T J Millar[2] and V Enea[1]

[1] Sifi SpA., via E. Patti, 36 95020 Aci S. Antonio (CT), Italy
[2] School of Science, Food and Horticulture, Parramatta Campus, Science Building, University of Western Sydney, Sydney, Australia

E-mail: f_miano@sifi.it

Received 13 February 2004
Published 18 June 2004
Online at stacks.iop.org/JPhysCM/16/S2461
doi:10.1088/0953-8984/16/26/019

Abstract

The outer interface of a tear film was studied with the aid of a model system able to investigate the interfacial phenomena derived from the spreading of an insoluble lipid multilayer onto a tear-like aqueous fluid. The interactions of such a layer with proteins dissolved in the aqueous phase beneath were also investigated. Emphasis was given to evaporation phenomena because the increased rate of tear evaporation in humans is often related to a number of ocular dysfunctions. The model tear was studied as a pendant drop that permitted a functional evaluation of the effect of lipids and proteins upon the evaporation of water from the tear film.

1. Introduction

The tear film acts as an interface between the ocular epithelium and the outside environment. It supplies a smooth, high-quality refractive surface over the cornea necessary for sharp, clear vision. Tears also serve as a vehicle for oxygenation and nourishment of the corneal surface and contain proteins with antimicrobial activity. Structurally tear film comprises three distinct layers, each essential for the physical integrity of the eye surface (figure 1). The innermost layer is made of mucous and is responsible for the 'wettability' of the tears, the middle layer is an aqueous solution containing proteins and salts and is produced by the lachrymal glands, and the outer layer is made of lipids produced by the meibomian glands, it enhances the stability of the tear film by reducing surface tension and retarding evaporation. A deficit in any one of these layers can result in a clinical condition known as 'dry eye'. Abnormal evaporation of tear fluid may arise from composition effects at the aqueous/lipid/air interface and from tear protein and lipids interactions.

1.1. Evaporation model

The evaporation from and condensation on a liquid phase have long been an important subject of fundamental research in various fields of physics, chemistry, meteorology and engineering.

 © 2004 IOP Publishing Ltd Printed in the UK

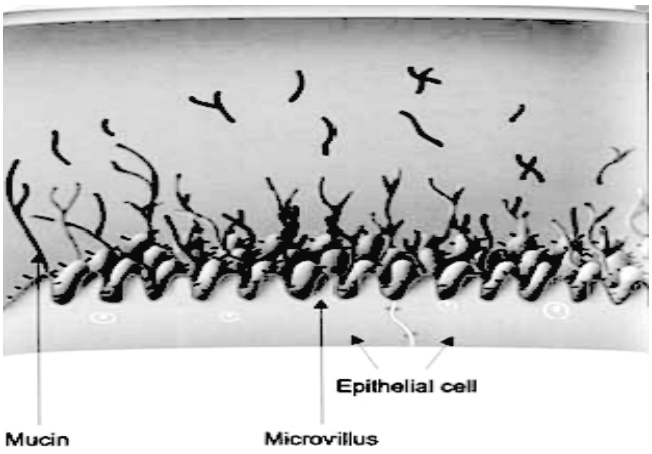

Figure 1. Schematic representation of tear film: the upper layer is lipid-rich (1×10^{-7} m); in the aqueous layer underneath proteins and inorganic ions are dissolved (7×10^{-6} m) and the lower layer is adherent to the ocular epithelium (1×10^{-6} m).

Since the pioneering work of Hertz [1] and Knudsen [2] on the evaporation of liquid mercury into a vacuum, both evaporation and condensation processes were treated on the basis of the kinetic theory of gases. In this case the focus is on the evaporation of an aqueous fluid in contact with its vapour at a given temperature. The evaporative flux is driven by the difference in the concentration of water at the liquid–vapour boundary and the equilibrium vapour concentration. The evaporation is also affected by the frictional velocity that accounts for the presence of air flux or wind. Moreover, heat exchange between the liquid and the vapour phase that produces surface cooling and differences in temperature are always present to some extent between the liquid bulk and the environment and should be considered. For the 10^{-6} m thick tear film, there is an additional complexity due to a temperature differential created by the eyeball (36 °C) and the ambient temperature.

A simplified evaporation model, in which constant temperature and humidity conditions are assumed, may be obtained from an equation analogous of Fick's first law for mass (m) transport [3]:

$$-\left(\frac{\mathrm{d}m}{\mathrm{d}t}\right) = AD\left(\frac{\mathrm{d}C_\mathrm{w}}{\mathrm{d}x}\right) \tag{1}$$

where A is the evaporating surface area, D is the diffusion coefficient of water vapour in air and C_w is the water vapour concentration at a distance x from the liquid–air boundary. D and C_w depend on temperature and their values are available in several databases. The evaporation rate may be measured in terms of evaporative flux J_w per area unit (equation (2)):

$$J_\mathrm{w} = \frac{\rho}{A}\left(\frac{\mathrm{d}V}{\mathrm{d}t}\right) \tag{2}$$

where ρ is water density and volume (V) variations are monitored with time. The evaporation rate may be correlated with the factors constituting equation (1) and then approximated to a finite difference equation (3):

$$J_\mathrm{w} = \frac{D}{x}(C_\mathrm{w} - C_\mathrm{d}) \tag{3}$$

where x is the effective boundary-layer thickness, within which the vapour concentration is assumed to linearly decrease from the full saturation value C_w to the environmental value C_d.

The thickness of the boundary layer is closely related to the airflow velocity profile around the liquid surface. For laminar airflow, the boundary-layer thickness is inversely related to the bulk airflow velocity. This thickness is difficult to measure and was estimated to be in the range of 2×10^{-3} m under a stagnant vapour phase. Equation (3) may be rewritten expressing the water vapour concentrations in terms of relative humidity (RH):

$$J_{\mathrm{w}} = \frac{DC_{\mathrm{w}}}{x} \frac{(100 - \mathrm{RH})}{100}. \tag{4}$$

The coefficient of equation (4) DC_{w}/x is defined as the reciprocal of the total evaporation resistance (R_{w}). In the case where the surface is coated by a lipid monolayer or multilayer the evaporation or permeability resistance will also include the contribution $1/R_{\mathrm{m}}$ of the spread film.

Assuming that the lipid layer contribution to evaporation resistance is additive [4] equation (4) becomes (5)

$$J_{\mathrm{m}} = \frac{1}{R_{\mathrm{w}} + R_{\mathrm{m}}} \frac{(100 - \mathrm{RH})}{100}. \tag{5}$$

The performance of the lipid layer spread at the boundary of the aqueous solution may be calculated as the ratio between the evaporation rate with the lipid layer present and that of the water-free surface:

$$\phi = J_{\mathrm{m}}/J_{\mathrm{w}}. \tag{6}$$

Combining (5) and (6) we obtain

$$(1 - \phi) = \frac{R_{\mathrm{m}}}{R_{\mathrm{w}} + R_{\mathrm{m}}} \tag{7}$$

which is a simple way to measure the effectiveness of a spread lipid layer in preventing the evaporation of water from the liquid subphase at a given temperature. The calculation of $(1 - \phi)$ from experimental data will be a basis for the comparison of different natural and artificial coatings of the tear aqueous phase.

The effectiveness of the lipid layer in retarding evaporation will depend on the surface concentration of lipids and on their nature. A tightly packed film will be most effective in reducing water permeation across the liquid–vapour boundary and the surface pressure Π is directly related to the surface density of the lipids at the interface.

Methods for measuring evaporation resistance have been reviewed in [5] and are divided into those that utilize a surface film balance, able to manipulate monolayers, and those in which the area of the surface is fixed. The novel measurement device set up for this purpose has the advantage of controlling both parameters at the same time and consists in a pendant drop apparatus in which a drop is hanging in a closed chamber with a stagnant environment where temperature and *relative humidity* are kept constant so that a steady state evaporation can be monitored together with the surface tension γ. A more detailed description of the device and procedure is reported in the experimental section. The effect of the lipids secreted by the meibomian gland on the evaporation rate was investigated and compared to pure lipid monolayers. The presence of tear proteins in solution was also studied in terms of protein adsorption at the interface and their effect on the evaporation rate.

2. Materials and methods

The model tear is represented by an aqueous solution of HBSS (Sigma), the composition of which is the following: $CaCl_2{\cdot}H_2O$, 0.19 mg ml^{-1}; $MgSO_4$, 0.098 mg ml^{-1}; KCl,

0.40 mg ml^{-1}; H_2PO_4, 0.06 mg ml^{-1}; $NaHCO_3$, 0.35 mg ml^{-1}; NaCl, 8.0 mg ml^{-1} and D-glucose 1.0 mg ml^{-1}. Lactoferrin (LF) of human origin, lysozyme (LYZ), dipalmitoyl phosphatidylcholine (DPPC), cholesteryl palmitate (CHP) chloroform and inorganic salts were purchased from Sigma (Italy) at their highest degree of purity.

2.1. Lipids collection

Meibomian gland secretion was sampled from the eyelid of the bovine conjunctiva obtained from a slaughterhouse. The material was obtained by gently squeezing the lid borders. The samples were dissolved in chloroform, centrifuged and evaporated in a rotating evaporator at 25 °C for 10 min. After determining the weight of the sampled lipids the product was redissolved in chloroform at a concentration of 0.5 mg ml^{-1}.

2.2. Measurement device

The measurements were carried out on a OCA20 (Dataphysics) optical contact angle equipped with two electronically driven Hamilton syringes, one for delivery of the aqueous phase and the second for the displacement of the lipid solution that spread concurrently with solvent evaporation. The drops were kept in a temperature controlled chamber. Temperature and RH were maintained constant by means of an external jacket circulating fluid and exposing saturated solutions of LiCl (15% RH), $NaNO_2$ (45% RH) and Na_2HPO_4 (95% RH) in the measurement chamber. RH was measured by a humidity sensor Sekonic RV1200 to ensure that steady conditions were matched. The surface tension is calculated applying the Young–Laplace equation (8), supposing axial symmetry of the drop's two-dimensional image recorded at regular intervals by a LCD camera:

$$\Delta P = \gamma\left(\frac{1}{R_1} + \frac{1}{R_2}\right). \tag{8}$$

Data processing yields the drop volume and surface; the surface tension γ; R_1 and R_2, the principal radii of curvature and ΔP, the difference in pressure along the interface.

2.3. Evaporation rate test

The following procedure is one from a typical experiment: a 15 μl HBSS solution drop is dispensed and volume surface tension (γ) and geometrical parameters of the drop (V, A) are monitored. Then 0.5 μl of lipid solution in chloroform ($C = 500$ μg ml^{-1}) is dispensed just upon the drop surface from the auxiliary syringe with the aid of a micromanipulator. In some experiments 2 μl of protein solution were also injected into the drop bulk. The drop geometrical parameters were monitored, starting just after the drop was equilibrated. RH was maintained steady by the exposure of a saturated salt solution. The evaporation rates were calculated from equation (7) in the range of $\Pi = 25$–35 mN m^{-1}, corresponding to the physiological value measured for tears [6].

3. Results

The evaporation experiments carried out at several RH and at 25 and 36 °C are representative of environmental and physiological temperatures. The evaporation rates have been reported with their regression lines in figure 2. Data variability originating from RH fluctuations with some saline saturated solutions do not compromise the linear fittings since in all cases the correlation

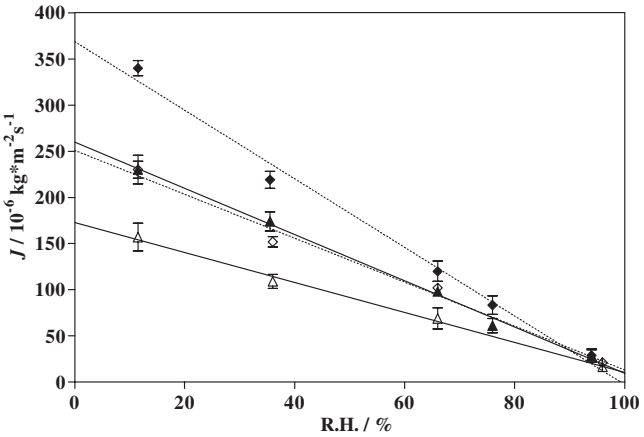

Figure 2. Evaporative flux versus relative humidity plot. Open symbols stand for $T = 25\,^{\circ}$C, full symbols for $T = 36\,^{\circ}$C, rhombuses are HBSS evaporating drops and triangles are HBSS in the presence of a meibomian lipid layer. Error bars refer to 95% confidence interval.

Table 1. Summary of evaporation parameters estimated from the experiments. The resistances R_m reported are referred to close-packed layers ($\Pi = 25$–35 mN m^{-1}).

			Meibomian lipids		DPPC		CHP	
T (°C)	$R_w^{(calc)}$ (m^2 s kg^{-1})	R_{HBSS} (m^2 s kg^{-1})	R_m (m^2 s kg^{-1})	$(1-\phi)$	R_{DPPC} (m^2 s kg^{-1})	$(1-\phi)$	R_{CHP} (m^2 s kg^{-1})	$(1-\phi)$
25	4270	4200	1960	0.318	467	0.100	—	<0.02
36	2190	2693	1174	0.304	312	0.104	66	0.024

factor is higher than 0.995. Evaporation resistances were calculated from the gradient and compared to those calculated for water from equation (4). The results are reported in table 1.

The relative decrease in evaporation rate in the presence of meibomian lipids $(1-\phi)$ is rather constant in the temperature range tested. The R_w calculated at 36 °C is lower than the experimental value probably because the cooling effect due to the heat of vaporization was not taken into account. In other words the drop while evaporating maintains a temperature that is near to 34 °C, rather than 36 °C. Compositional analysis of meibomian lipids showed that the principal bands are phospholipids, cholesterol, trisearitin, linoleic acid, triolean and cholesteryl palmitate, in agreement with the literature [7].

The effect of surface pressure on the evaporation rate is reported in figure 3 where the DPPC and meibomian lipid film are compared: it can be observed that the increase of Π produces a reduction of the evaporative flux J_w. In detail, in the case of DPPC, J_w reduces from its initial value at $\Pi \approx 12$–15 mN m^{-1}, where a condensed monolayer is established, and remains steady up to the monolayer collapse ($\Pi \approx 45$ mN m^{-1}); the Π range at which J_w decreases is 6–8 mN m^{-1}.

Finally, the effect of protein adsorption in the meibomian lipid layer is shown in figure 4 as Π versus $\Delta\Pi$ plotted lines. Both proteins (LYZ and LF) were found to insert at the liquid–air interface since $\Delta\Pi > 0$. They were excluded from the interface at a surface pressure of 32.5 mN m^{-1} (LYZ) and 34 mN m^{-1} (LF), higher than the surface pressure of whole tears, which is ∼25 mN m^{-1} [6]. The insertion of proteins into the lipid layer caused a reduction in the resistance against the evaporative flux: $(1-\phi)$ was 0.250 for LYZ and 0.260

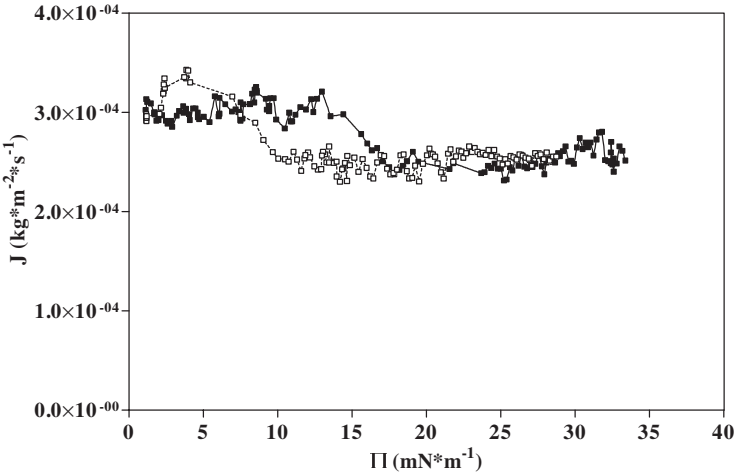

Figure 3. Evaporation rate of a HBSS drop coated with meibomian lipid layer (open squares) and DPPC (full squares) versus surface pressure Π at $T = 36\,^{\circ}\mathrm{C}$ and RH = 15%. Data are collected at a rate of 4 points min^{-1}.

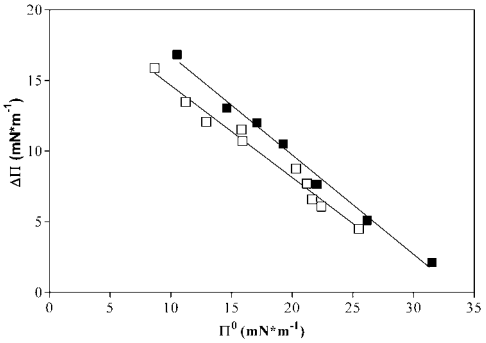

Figure 4. Surface pressure plot of meibomian lipid–air surface pressure at 36 °C in the presence of LYZ (open squares) and LF (full squares) in the aqueous subphase.

for LF mixed layers. The addition of proteins did not have any effect on the evaporation rate of a HBSS drop.

4. Discussion

The pendant drop was shown to be a valuable model, representative of tears for the study of interfacial phenomena. The small size of the system allowed testing of biological samples and the control of a number of physical parameters that permitted simulation of tear evaporation.

The nature of the evaporation process and the type of information required to assess the efficacy of the meibomian lipid layer in retarding tear evaporation have been described with simplified diffusion equations. However, caution should be observed in using these equations if the drop cooling caused by the latent heat of evaporation significantly reduces the actual temperature of the interface.

Since the relative decrease in the evaporation rate was shown to be independent of the temperature and water vapour density in the range of interest, it suffices to perform evaporation

experiments just at one given condition and then to calculate the ratio of evaporative flux between the aqueous phase with and without a spread lipid layer. In this way the effectiveness of that lipid or lipid mixture in offering resistance against evaporation can be assessed. Experimental data for the retardation of evaporation have shown that the meibomian lipid mixture is more effective than the sum of its individual components and that the protein effect on the evaporative process results in a moderate reduction of the evaporation resistance. Both observations may be explained assuming that evaporation is restricted to the portion of surface that is not occupied by insoluble molecules. It can be expected that the two-dimensional packing of a mixture is more efficient in obstructing the greater part of the exposed surface than the arrangement of a single substance monolayer. Moreover, protein intrusion into the surface, similar to surfactants [8], creates lipid-free domains through which the water molecules are more easily transported into the vapour phase.

At physiological conditions the surface pressure of tears (20–25 mN m^{-1}) is below the exclusion pressure of the lipid layer versus most of the tear proteins. From the dynamics of protein adsorption, it was found that the formation of a mixed lipid–protein interface takes place in less than a minute. Therefore, since eye blinks occur at a frequency of 20–50 s, this implies that proteins are displaced from the tear surface and permit the restoration of a full lipid layer.

Finally, it is worth noting that tear evaporation is affected to a greater extent by environmental factors (i.e. T and RH) than physiological ones. However, pathological alteration of the tear film may produce a significant increase of the evaporative flux. Future experiments, with meibomian lipids sampled from 'dry eye' patients will be undertaken to investigate this hypothesis.

References

[1] Hertz H 1882 *Ann. Phys.* **17** 177
[2] Knudsen M 1915 *Ann. Phys.* **352** 697
[3] Ginsberg L and Gershfeld N L 1985 *Biophys. J.* **47** 211–5
[4] Barnes G T 1993 *J. Hydrol.* **145** 165–73
[5] Barnes G T 1986 *Adv. Colloid Interface Sci.* **25** 89–200
[6] Holly F J 1974 *J. Colloid Interface Sci.* **49** 221–31
[7] Shine W E and McCulley J P 2003 *Curr. Eye Res.* **26** 89–94
[8] Lunkenheimer K and Zembala M 1997 *J. Colloid Interface Sci.* **188** 363–71